THE JOURNAL OF PHYSICAL CHEMISTRY Letters

Letter

Cite This: J. Phys. Chem. Lett. 2018, 9, 1284−1289

pubs.acs.org/JPCL

Dipole-Bound Anions of Intramolecular Complexes

Elena F. Belogolova,[§,†] Gaoxiang Liu,[§,‡] Evgeniya P. Doronina,[†] Sandra M. Ciborowski,[‡] Valery F. Sidorkin,[*,†] and Kit H. Bowen[*,‡]

[†]A. E. Favorsky Irkutsk Institute of Chemistry, Siberian Branch of the Russian Academy of Sciences, Favorsky, 1, Irkutsk 664033, Russian Federation

[‡]Department of Chemistry, Johns Hopkins University, Baltimore, Maryland 21218, United States

Supporting Information

ABSTRACT: Dipole-bound molecular anions are often envisioned as unperturbed neutral, polar molecules with single excess electrons. We report the observation of intramolecular structural distortions within silatrane molecules due to the formation of their dipole-bound anions. The combination of Rydberg electron transfer−anion photoelectron spectroscopy (RET-PES) and ab initio computational methodologies (CCSD and MP2) was used to study 1-hydro- (**HS**) and 1-fluoro- (**FS**) silatranes and their dipole bound anions, HS^- and FS^-. The vertical detachment energies (VDEs) of HS^- and FS^- were measured to be 48 and 93 meV, respectively. Ab initio calculations accurately reproduced these VDE values as well as their photoelectron spectral profiles. This work revealed significant shortening (by ∼0.1 Å) of dative Si ← N bond lengths when **HS** and **FS** formed dipole-bound anions, HS^- and FS^-. Detailed computational (Franck−Condon) analyses explained the absence of vibrational features in the photoelectron spectra of HS^- and FS^-.

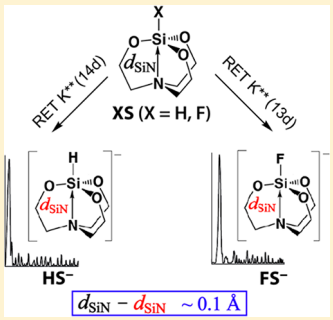

Dipole-bound anions can be formed by the interaction of electrons with highly polar neutral molecules or small clusters.[1−6] The formation of dipole-bound states is thought to be the initial step in the attachment of electrons to many polar molecules. Thus dipole-bound anions that play this role are sometimes referred to as "doorway" or "stepping stone" states.[7−16] A combination of experimental findings and theoretical predictions implies that molecules with dipole moments greater than 2.5 D can form dipole-bound anions.[17,18]

The excess electron in a dipole-bound molecular anion can be envisioned as a highly delocalized cloud, tethered at the positive end of the molecular dipole and extending over a relatively large volume. Because it interacts only weakly with the larger molecule, the excess electron's binding energy is very small, and there is little distortion of the molecule's nuclear framework. For these reasons, dipole-bound anions exhibit a distinctive anion photoelectron spectroscopic signature, consisting of a single narrow peak at very low electron binding energy (EBE).[19,20] The narrow peak derives from the fact that the structures of dipole-bonded molecular anions are essentially the same as their corresponding neutral molecules, which, in turn, leads to near-perfect Franck−Condon overlap and thus to a single narrow peak. In cases where significant structural distortion does occur, however, additional peaks can appear in the anion photoelectron spectra. These are often seen in the dipole-bound anions of hydrogen bond, dimers, and trimers, such as $(HF)_2$[21,22] and indole$(H_2O)_{1,2}$,[16] where intermolecular structural changes have occurred. Such peaks are due to combination bands of molecular and intermolecular (weak) vibrations. The dipole-bound anions of lone molecules do not show clear evidence of structural distortion; that is, they tend to exhibit single narrow peaks in their anion photoelectron spectra without evidence of additional Franck−Condon combination bands.

Silatranes, $XSi(OCH_2CH_2)_3N$ (see Figure 1), are highly polar (∼6−9 D) molecular cages with labile, internal Si ← N dative bonds. These bonds are strongly sensitive to the nature of their axial substituents, X, and to external factors.[23−27] An attractive interaction Si ← N in silatranes predetermines the peculiarity of their structure, unusual spectral characteristics, and reactivity as well as a wide spectrum of biological activity.[23,24]

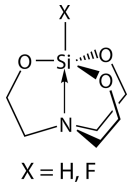

Figure 1. Structure of 1-hydro- (**HS**) and 1-fluoro- (**FS**) silatrane.

Here we present results from our combined experimental−theoretical study of 1-hydro-silatrane (**HS**) and 1-fluoro-silatrane (**FS**) and their anions. These two were initially selected because they do not have low-lying vacant orbitals (primarily of π-type)[25−28] and therefore are candidates for forming dipole-bound anions, HS^- and FS^-. It is also important to note that **HS** and **FS** differ in their Si ← N bond

Received: February 2, 2018
Accepted: February 26, 2018
Published: February 26, 2018

ACS Publications © 2018 American Chemical Society

DOI: 10.1021/acs.jpclett.8b00355
J. Phys. Chem. Lett. 2018, 9, 1284−1289

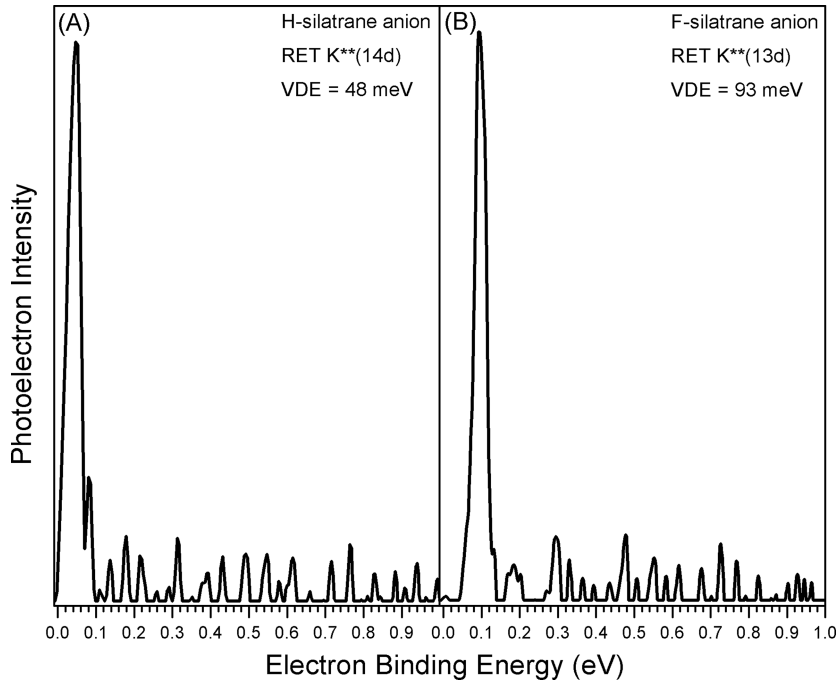

Figure 2. Anion photoelectron spectra of the dipole-bound anions of (A) 1-hydro- and (B) 1-fluoro-silatrane measured with the first harmonic of a Nd:YAG laser (1064 nm, 1.165 eV).

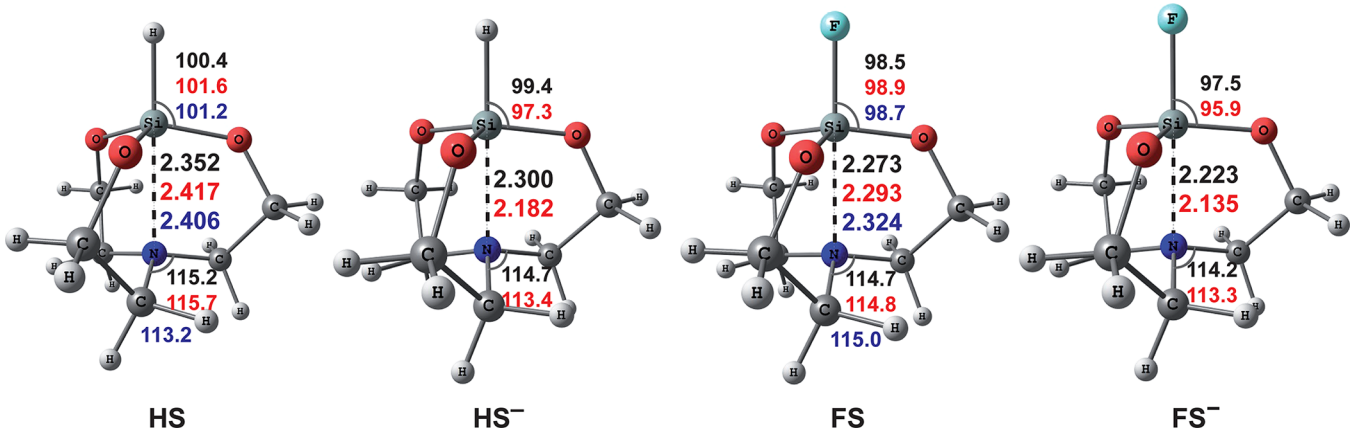

Figure 3. MP2/B2(s) (in black) and CCSD/6-31++G(d,p) (in red) optimized geometries of silatranes, **HS** and **FS**, and their dipole-bound anions, HS^- and FS^-. Electron diffraction structural parameters for **HS** and **FS** are shown in blue. The bond lengths are in angstroms and the bond angles are in degrees. B2(s) is the 6-311++G(d,p) triple-ζ basis set augmented with an additional diffuse s function on each H atom and a set of diffuse s and p functions on the other atoms (see further description in the Supporting Information).

strengths[23,25] and that their geometries are known from electron diffraction studies.[29,30]

The formation of the anions HS^- and FS^- benefited from our use of specialized experimental methods. Rydberg electron transfer (RET) is the ideal technique for forming dipole-bound anions. Schermann, Compton, Hammer, and ourselves have used RET extensively to prepare dipole-bound anions and analyze their EBEs using a semiempirical formula.[17,18,31−33] The recently developed combination of RET and anion photoelectron spectroscopy (PES), however, provides a somewhat more comprehensive picture of dipole-bound anion energetics and structural aspects. In this work, we used our one-of-a-kind RET-PES apparatus and state-of-the-art ab initio computational methods to study the dipole-bound anions of 1-hydro- (**HS**) and 1-fluoro- (**FS**) silatrane, that is, HS^- and FS^-.

Silatrane anions, HS^- and FS^-, were generated by a RET source. Neutral silatrane molecules, **HS** and **FS**, were vaporized in a heated pulsed valve and expanded with 10 psig of helium gas. Their anions, HS^- and FS^-, were formed when the neutral **HS** and **FS** molecules collided with a thermally expanded beam of potassium atoms, which had been excited to *n*d Rydberg states, where *n* is the principal quantum number, in two steps using two dye lasers. The anion signals were found to optimize at the 14d Rydberg state for HS^- and 13d Rydberg state for FS^-. The anions were then extracted into a time-of-flight mass spectrometer and mass-selected, after which their excess electrons were photodetached with another laser and energy-analyzed using velocity-map imaging spectroscopy. Details of the experiments are presented in the Supporting Information.

Figure 2 presents the anion photoelectron spectra of HS^- and FS^-. The comb-like spikes along the baseline are due to

DOI: 10.1021/acs.jpclett.8b00355
J. Phys. Chem. Lett. 2018, 9, 1284−1289

noise and are of no consequence. Each spectrum consists of a major, sharp peak at rather low EBE, strongly implying that **HS**$^-$ and **FS**$^-$ are dipole-bound anions. For **HS**$^-$, the EBE peak is centered at 48 meV with a full width at half-maximum (fwhm) of ∼35 meV (Figure 2A). The EBE peak of **FS**$^-$ is centered at 93 meV also with an fwhm of ∼35 meV (Figure 2B), 35 meV being only slightly greater than the experimental resolution. We assign these two peaks as the origins of the transitions between the dipole-bound anions and their corresponding neutral molecules. Therefore, the vertical detachment energy (VDE) values for **HS**$^-$ and **FS**$^-$ anions are 48 and 93 meV, respectively. Note that the EBE value of **FS**$^-$ is higher than that of **HS**$^-$, which is to be expected due to the higher dipole moment of **FS** as compared with **HS** (Table S1). In photoelectron spectra such as these, which are dominated by single sharp peaks due to the close similarity between the structures of the anion and its neutral counterpart, the anion's VDE value is only slightly greater than the value of its corresponding neutral's electron affinity (EA).

The computed C_3 symmetry structures of **HS**, **FS**, and their dipole-bound anions, **HS**$^-$ and **FS**$^-$, optimized at MP2/B2(s) and CCSD/6-31++G(d,p) levels of theory are presented in Figure 3. Both the $^2A_1$ dipole-bound anions and their corresponding neutral molecules were all found to exhibit single minima on their potential energy surfaces. For neutral molecules, the CCSD/6-31++G(d,p) method accurately reproduces the Si ← N bond lengths, $d_{Si\leftarrow N}$, as determined from electron diffraction data[29,30] to within ∼0.03 Å, while with the MP2/B2(s) method, the discrepancy is ∼0.05 Å. More importantly, regardless of the method used for geometry optimization, a significant deformation of the coordination center around the silicon atom, $XSiO_3N$, is observed upon the addition of an excess electron. This is also accompanied by an increase in η_e, that is, the pentacoordinate character or trigonal bipyramidal structure of the silicon atom (Figure 3, Table S2). Such structural deformation is mainly manifested by a decrease in $d_{Si\leftarrow N}$ in the anion compared with that of its corresponding neutral. So, as a measure of the silatrane geometry response to the extra electron addition, we have chosen the $\Delta d_{Si\leftarrow N}$ value, which is defined as the difference between the experimental Si ← N bond lengths for neutral molecules and the calculated bond lengths for their dipole-bound anions. For **HS**$^-$, $\Delta d_{Si\leftarrow N}$ is predicted to be 0.106 Å when calculated by the MP2/B2(s) method and 0.224 Å when computed by the CCSD/6-31++G(d,p) method. For **FS**$^-$, $\Delta d_{Si\leftarrow N}$ is computed to be 0.101 Å by MP2/B2(s) and 0.189 Å by CCSD/6-31++G(d,p) (see Figure S1, its legend and corresponding comments).

It is pertinent to note that upon the formation of valence-bound silatrane anions, calculations show their dative Si ← N bonds elongating rather than shortening.[34]

Figure 4 shows that the spin density in **HS**$^-$ and **FS**$^-$ is localized outside the nuclear frame on the positive dipole end, confirming them as dipole-bound anions (see also the Figure S2). Therewith, in accordance with the dipole moment values in **HS** and **FS**, the electron cloud density for **FS**$^-$ is higher than that for **HS**$^-$ (see, for example, ref 35).

The experimental and calculated VDE values for the dipole-bound anions, **HS**$^-$ and **FS**$^-$, are presented in Table 1. The MP2/aug-cc-pVDZ+5s5p4d(N) and MP2/aug-cc-pVDZ +5s5p(H_3) methods predict negative VDE values, incorrectly estimating the stability of the dipole-bound anions. Only methods that invoke basis sets with a large number of diffuse functions or account for more electron correlation give

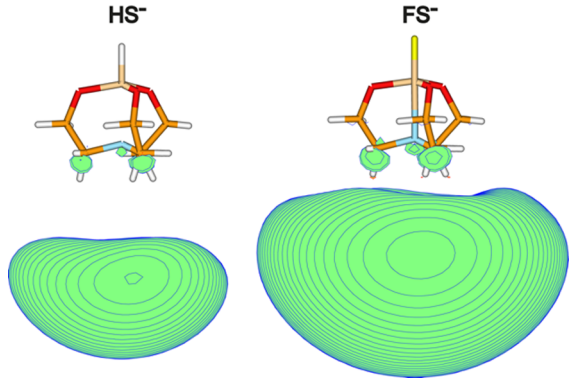

Figure 4. Spin density distributions of **HS**$^-$ and **FS**$^-$ obtained at the MP2/B2(s) level (plotted with 0.00003 e·bohr^{-3} contour spacing).

Table 1. Experimental and Calculated Values of the Vertical Detachment Energies (VDEs, in eV) for the Dipole-Bound Anions, HS$^-$ and FS$^-$[b]

Geometry	CCSD/6-31++G(d,p)		MP2/B2(s)	
Energy	**HS$^-$**	**FS$^-$**	**HS$^-$**	**FS$^-$**
Exp.	**0.048**	**0.093**	**0.048**	**0.093**
MP2/aug-cc-pVDZ+5s5p4d(N)	-0.003	0.001	-0.005	-0.001
MP2/aug-cc-pVDZ+5s5p(H_3)	-0.004	-0.004	-0.005	-0.004
MP2/aug-cc-pVDZ+5s5p4d(H_3N)	0.050	0.094	0.031	0.072[a]
MP2/B2(s)	0.047	0.089	0.031	0.068
MP2/B2	0.052	0.099	0.033	0.075
CCSD/B2(s)	0.063	0.111	0.042	0.086
CCSD(T)/B2(s)	0.066	0.115	0.045	0.089
CCSD/B2	0.068	0.120	0.045	0.094
CCSD(T)/B2	0.071	0.123	0.048	0.097

[a]The same VDE value was obtained using the MP2/aug-cc-pVDZ +7s7p8d(N) method. [b]Red boxes encapsulate the combinations of theoretical methods for geometry and energies that best match experiment.

qualitatively correct predictions on electron attachment to these molecules. Exceptional agreement with experimental VDE values is observed when using the CCSD/6-31++G(d,p) geometries with MP2/aug-cc-pVDZ+5s5p4d(H_3N) and MP2/B2(s) methods. On the contrary, for MP2/B2(s) geometries, the best quality VDE calculations are demonstrated by using CCSD and CCSD(T) methods with the B2(s) and B2 basis sets. Noticeably, the EAs of **HS** and **FS** are calculated at the CCSD(T)/B2 level to be 39 and 90 meV, respectively, these being slightly lower than their VDE values, as expected. Because the VDE and EA values virtually coincide when there is near-perfect Franck−Condon overlap, as is the case for dipole-bound anions, the EA values of **HS** and **FS** were not separately determinable by the experiment.

The $\Delta d_{Si\leftarrow N}$ values predicted by CCSD/6-31++G(d,p) are considerably larger than those predicted by MP2/B2(s), specifically by 0.108 Å for **HS**$^-$ and 0.088 Å for **FS**$^-$ (see Figure 3). Because excellent agreement between the experimental and calculated VDE values is found for both MP2 and CCSD optimized geometries, it is difficult to determine which geometry is more accurate based only on the quality of the VDE calculations.

DOI: 10.1021/acs.jpclett.8b00355
J. Phys. Chem. Lett. 2018, 9, 1284−1289

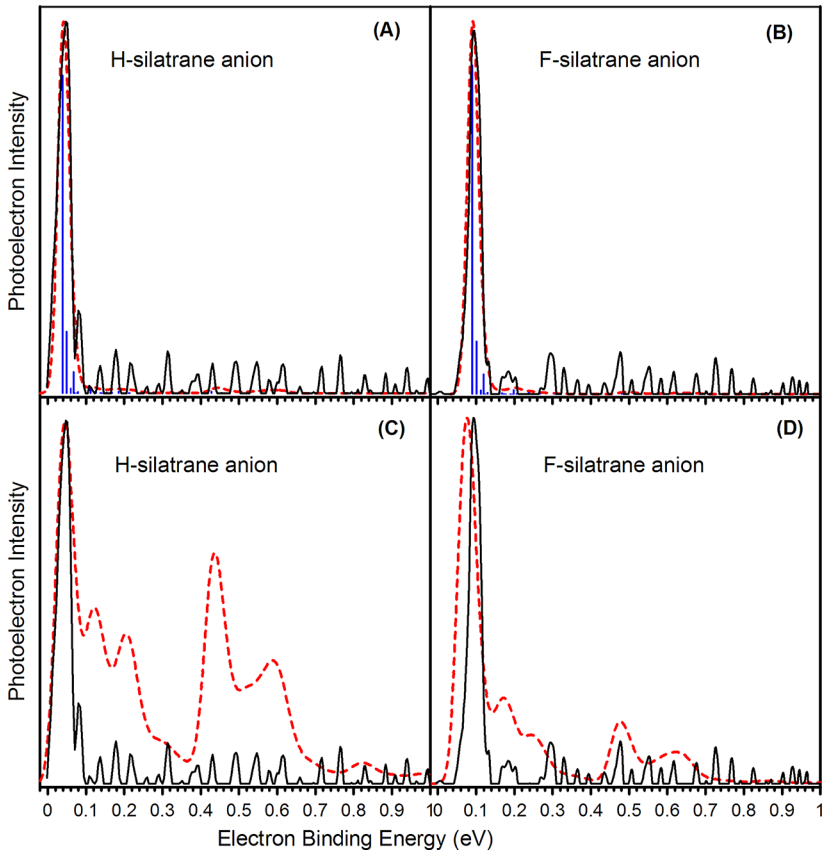

Figure 5. Overlaid experimental (black solid line) and Franck−Condon (red dashed line) photoelectron spectra of HS^- and FS^-. Vibrational progressions are given by a blue line spectrum. (A,B) MP2/B2(s) geometry optimizations and normal vibrational modes. In determining the position of the 0−0 transition, we used the CCSD(T)/B2 adiabatic electron affinity (AEA) value (0.039 eV) for HS^- and the CCSD/B2 AEA value (0.090 eV) for FS^-. (C,D) CCSD/6-31++G(d,p) optimized geometries and MP2/B2(s) normal vibrational modes.

The choice between the geometry optimization methods for silatranes and their anions can also be done using the Franck−Condon simulation of the photoelectron spectra of HS^- and FS^- (Figure 5). An excellent match between experimental and theoretical photoelectron spectra is achieved when using the MP2 optimized geometries for HS^- and FS^- (Figure 5A,B). The estimated fwhm values for the dominant peak in the theoretical photoelectron spectra of HS^- and FS^- (0.036 and 0.035 eV, respectively) agree with the experimental widths. The simulated photoelectron spectra of HS^- and FS^- using the CCSD geometries have complex vibrational profiles, which are fundamentally different from the observed experimental photoelectron spectra (Figure 5C,D). As a result, we conclude that the CCSD/6-31++G(d,p) method overestimates the change of the Si ← N bond length and also other structural parameters when an excess electron is attached to **HS** or **FS**. The MP2/B2(s) level of theory predicts more accurate anionic geometries and reasonable $\Delta d_{Si\leftarrow N}$ values of 0.106 Å for HS^- and 0.101 Å for FS^-. Such a large deformation of bond contacts is unprecedented for dipole-bound molecular anions.

Franck−Condon factors are listed in Table S3. We show that the main peaks in the simulated photoelectron spectra of HS^- and FS^- are formed by the superposition of the 0_0^0, 1_0^1, 4_0^1 and 0_0^0, 1_0^1, 6_0^1 transitions, respectively. These transitions are spaced apart from one another by <0.03 eV, which is comparable to the instrumental resolution. This situation can explain the observed asymmetry and broadening at the bottom of the HS^- and FS^- peaks on their high EBE sides. The geometric relaxation upon the attachment of an electron occurs mainly along the first and fourth normal vibrational modes in **HS** and along the first and sixth modes in **FS**. They correspond to the Si ← N dative bond stretching and torsional motion of the SiO_3 and $N(CH_2)_3$ fragments around the C_3 symmetry axis in the silatrane molecule. The corresponding harmonic vibrations have very low frequencies (ω): for **HS**, ω_1 = 85 cm^{-1} and ω_4 = 235 cm^{-1} with increases of 2 and 10 cm^{-1}, respectively, upon transition to the anionic state; for **FS**, ω_1 = 91 cm^{-1} and ω_6 = 237 cm^{-1} with increases of 0 and 14 cm^{-1}, respectively, in the anionic state. The reason for this is the high lability of the Si ← N dative bond in **HS**, **FS**, and their dipole-bound anions, where <0.017 eV of energy is needed to change the Si ← N distance by 0.1 Å (see Figure S1 and refs 36−38). Consequently, the vibrational transitions (0_0^0, 1_0^1, 4_0^1) and (0_0^0, 1_0^1, 6_0^1), which are associated with the donor−acceptor moiety $XSiO_3$ ← $N(CH_2)_3$, are very energetically close and form a separate, narrow main peak (typical of dipole bound anions) in the photoelectron spectra of HS^- and FS^-.

In addition to the above, the vibrational transitions 13_0^1 at 0.11 eV and 33_0^1 at 0.19 eV for HS^- and 22_0^1 at ∼0.20 eV for FS^- were observed in their theoretical spectra (Table S3). However, despite the significant structural changes in the coordination center $XSiO_3N$ of **HS** and **FS** upon the extra electron attachment, the intensity of these additional peaks in the photoelectron spectra of HS^- and FS^- does not exceed the noise level in the experimental spectrum. Indeed, judging from the Franck−Condon factors values (Table S3), the relatively

DOI: 10.1021/acs.jpclett.8b00355
J. Phys. Chem. Lett. 2018, 9, 1284−1289

rigid modes 13 (HSiO bending) and 33 (CO bond stretching) in **HS** and mode 22 (SiF bond stretching) in **FS** are practically not populated upon the electron photodetachment from $\mathbf{HS}^-$ and $\mathbf{FS}^-$.

To summarize, we report the observation of an unusual structural change when a lone molecule (intramolecular complex) forms dipole-bound anions. This provides new insight into our current understanding about dipole-bound anions, where excess electrons are weakly bound to the neutral molecular framework. The novel combination of RET and PES is promising for investigating anions that were not easily attained previously.

■ ASSOCIATED CONTENT

Supporting Information

The Supporting Information is available free of charge on the ACS Publications website at DOI: 10.1021/acs.jpclett.8b00355.

Detailed experimental and theoretical methods. Raw velocity map images. Table S1. Dipole moments of silatranes. Table S2. Experimental and calculated (at different theory levels) structural parameters of silatranes and their anions. Table S3. FC factors, intensities, and transition energies in the PES of silatrane anions. Figure S1. CCSD(T)/B2(s)//MP2/B2(s) energies of H- and F-silatranes and their anions as functions of the Si···N distance. Figure S2. SOMO of $\mathbf{HS}^-$ and $\mathbf{FS}^-$. Figure S3. Velocity map photoelectron images and anisotropy parameters for H- and F-silatrane. Cartesian coordinates of the molecules depicted in Figure 3. (PDF)

■ AUTHOR INFORMATION

Corresponding Authors

*V.F.S.: E-mail: svf@irioch.irk.ru.

*K.H.B.: E-mail: kbowen@jhu.edu.

ORCID

Gaoxiang Liu: 0000-0002-1001-0064

Evgeniya P. Doronina: 0000-0001-6663-061X

Sandra M. Ciborowski: 0000-0001-9453-4764

Valery F. Sidorkin: 0000-0002-8848-7567

Kit H. Bowen: 0000-0002-2858-6352

Author Contributions

§E.F.B. and G.L. contributed equally to this work.

Notes

The authors declare no competing financial interest.

■ ACKNOWLEDGMENTS

We are grateful to Dr. O. Trofimova and Dr. Y. Bolgolva for providing samples of 1-hydro- and 1-fluoro-silatranes. The experimental part of this material is based on work supported by the (U.S.) National Science Foundation (NSF) under grant no. CHE-1664182 (K.H.B.).

■ REFERENCES

(1) Jordan, K. D. Studies of the Temporary Anion States of Unsaturated Hydrocarbons by Electron Transmission Spectroscopy. *Acc. Chem. Res.* **1979**, *12*, 36−42.

(2) Simons, J.; Jordan, K. D. Ab Initio Electronic Structure of Anions. *Chem. Rev.* **1987**, *87*, 535−555.

(3) Gutowski, G.; Skurski, P.; Boldyrev, A. I.; Simons, J.; Jordan, K. D. Contribution of Electron Correlation to the Stability of Dipole-Bound Anionic States. *Phys. Rev. A: At., Mol., Opt. Phys.* **1996**, *54*, 1906−1909.

(4) Simons, J. Molecular Anions. *J. Phys. Chem. A* **2008**, *112*, 6401−6511.

(5) Liu, H. T.; Ning, C. G.; Huang, D. L.; Dau, P. D.; Wang, L. S. Observation of Mode-Specific Vibrational Autodetachment from Dipole-Bound States of Cold Anions. *Angew. Chem., Int. Ed.* **2013**, *52*, 8976−8979.

(6) Huang, D.; Liu, H.; Ning, C.; Zhu, G.; Wang, L. Probing the Vibrational Spectroscopy of the Deprotonated Thymine Radical by Photodetachment and State-Selective Autodetachment Photoelectron Spectroscopy via Dipole-Bound States. *Chem. Sci.* **2015**, *6*, 3129−3138.

(7) Dabkowska, I.; Rak, J.; Gutowski, M.; Nilles, J. M.; Stokes, S. T.; Radisic, D.; Bowen, K. H., Jr. Barrier-Free Proton Transfer in Anionic Complex of Thymine with Glycine. *Phys. Chem. Chem. Phys.* **2004**, *6*, 4351−4357.

(8) Chomicz, L.; Zdrowowicz, M.; Kasprzykowski, F.; Rak, J.; Buonaugurio, A.; Wang, Y.; Bowen, K. H. How to Find Out Whether a 5-Substituted Uracil Could Be a Potential DNA Radiosensitizer. *J. Phys. Chem. Lett.* **2013**, *4*, 2853−2857.

(9) Bachorz, R. A.; Klopper, W.; Gutowski, M.; Li, X.; Bowen, K. H. Photoelectron Spectrum of Valence Anions of Uracil and First-Principles Calculations of Excess Electron Binding Energies. *J. Chem. Phys.* **2008**, *129*, 054309.

(10) Xu, S. J.; Nilles, J. M.; Bowen, K. H. Zwitterion Formation in Hydrated Amino Acid, Dipole Bound Anions: How Many Water Molecules Are Required. *J. Chem. Phys.* **2003**, *119*, 10696−10701.

(11) Sommerfeld, T. Intramolecular Electron Transfer from Dipole-Bound to Valence Orbitals: Uracil and 5-Chlorouracil. *J. Phys. Chem. A* **2004**, *108*, 9150−9154.

(12) Eustis, S. N.; Radisic, D.; Bowen, K. H.; Bachorz, R. A.; Haranczyk, M.; Schenter, G.; Gutowski, M. Electron-Driven Acid Base Chemistry: Proton Transfer from Hydrogen Chloride to Ammonia. *Science* **2008**, *319*, 936−939.

(13) Sommerfeld, T. Doorway Mechanism for Dissociative Electron Attachment to Fructose. *J. Chem. Phys.* **2007**, *126*, 124301−124305.

(14) Desfrancois, C.; Baillon, B.; Schermann, J. P.; Arnold, S. T.; Hendricks, J. H.; Bowen, K. H. Prediction and Observation of a New, Ground State, Dipole-Bound Dimer Anion: The Mixed Water/Ammonia System. *Phys. Rev. Lett.* **1994**, *72*, 48−51.

(15) Kelly, J.; Xu, S.; Graham, J.; Nilles, M.; Radisic, D.; Buonaugurio, A.; Bowen, K.; Hammer, N.; Tschumper, G. Photoelectron Spectroscopic and Computational Study of Hydrated Pyrimidine Anions. *J. Phys. Chem. A* **2014**, *118*, 11901−11907.

(16) Buytendyk, A. M.; Buonaugurio, A. M.; Xu, S. J.; Nilles, J. M.; Bowen, K. H.; Kirnosov, N.; Adamowicz, L. Computational and Photoelectron Spectroscopic Study of the Dipole-Bound Anions, Indole$(H_2O)_{1,2}^-$. *J. Chem. Phys.* **2016**, *145*, 024301.

(17) Compton, R. N.; Hammer, N. I. *Adv. Gas Phase Ion Chem.*; JAI Press: Stamford, CT, 2001.

(18) Desfrancois, C.; Khelifa, N.; Lisfi, A.; Schermann, J. P.; Eaton, J. G.; Bowen, K. H. Electron Transfer Collisions Between Small Water Clusters and Laser-Excited Rydberg Atoms. *J. Chem. Phys.* **1991**, *95*, 7760−7762.

(19) Jordan, K. D.; Luken, W. Theoretical Study of the Binding of an Electron to a Molecular Dipole: $LiCl^-$. *J. Chem. Phys.* **1976**, *64*, 2760−2766.

(20) Castleman, A. W.; Bowen, K. H. Clusters: Structure, Energetics, and Dynamics of Intermediate States of Matter. *J. Phys. Chem.* **1996**, *100*, 12911−12944.

(21) Hendricks, J. H.; de Clercq, H. L.; Lyapustina, S. A.; Bowen, K. H. Negative Ion Photoelectron Spectroscopy of the Ground State, Dipole-Bound Dimeric Anion, $(HF)_2^-$. *J. Chem. Phys.* **1997**, *107*, 2962−2967.

(22) Gutowski, M.; Skurski, P. Theoretical Study of the Dipole-Bound Anion $(HF)_2^-$. *J. Chem. Phys.* **1997**, *107*, 2968−2973.

(23) Pestunovich, V.; Kirpichenko, S.; Voronkov, M. *The Chemistry of Organic Silicon Compounds*; Wiley: Chichester, U.K., 1998.

(24) Puri, J. K.; Singh, R.; Chahal, V. K. Silatranes: A Review on Their Synthesis, Structure, Reactivity and Applications. *Chem. Soc. Rev.* **2011**, *40*, 1791−1840.
(25) Belogolova, E. F.; Sidorkin, V. F. Correlation Among the Gas-Phase, Solution, and Solid-Phase Geometrical and NMR Parameters of Dative Bonds in the Pentacoordinate Silicon Compounds. 1-Substituted Silatranes. *J. Phys. Chem. A* **2013**, *117*, 5365−5376.
(26) Sidorkin, V. F.; Belogolova, E. F.; Doronina, E. P. Assignment of Photoelectron Spectra of Silatranes: First Ionization Energies and the Nature of the Dative Si←N Contact. *Phys. Chem. Chem. Phys.* **2015**, *17*, 26225−26237.
(27) Sidorkin, V. F.; Belogolova, E. F.; Wang, Y.; Jouikov, V.; Doronina, E. P. Electrochemical Oxidation and Radical Cations of Structurally Non-Rigid Hypervalent Silatranes: Theoretical and Experimental Studies. *Chem. - Eur. J.* **2017**, *23*, 1910−1919.
(28) Trofimov, A. B.; Zakrzewski, V. G.; Dolgounitcheva, O.; Ortiz, J. V.; Sidorkin, V. F.; Belogolova, E. F.; Belogolov, M.; Pestunovich, V. A. Silicon-Nitrogen Bonding in Silatranes: Assignment of Photoelectron Spectra. *J. Am. Chem. Soc.* **2005**, *127*, 986−995.
(29) Shishkov, I. F.; Khristenko, L. V.; Rudakov, F. M.; Golubinskii, A. V.; Vilkov, L. V.; Karlov, S. S.; Zaitseva, G. S.; Samdal, S. Molecular Structure of Silatrane Determined by Gas Electron Diffraction and Quantum-Mechanical Calculations. *Struct. Chem.* **2004**, *15*, 11−16.
(30) Forgács, G.; Kolonits, M.; Hargittai, I. The Gas-Phase Molecular Structure of 1-Fluorosilatrane from Electron Diffraction. *Struct. Chem.* **1990**, *1*, 245−250.
(31) Hammer, N.; Diri, K.; Jordan, K.; Desfrancois, C.; Compton, R. Dipole-Bound Anions of Carbonyl, Nitrile, and Sulfoxide Containing Molecules. *J. Chem. Phys.* **2003**, *119*, 3650−3660.
(32) Hammer, N.; Compton, R. N.; Adamowicz, L.; Stepanian, S. Isotope Effects in Dipole-Bound Anions of Acetone. *Phys. Rev. Lett.* **2005**, *94*, 153004.
(33) Hammer, N.; Hinde, R.; Compton, R.; Diri, K.; Jordan, K.; Radisic, D.; Stokes, S. T.; Bowen, K. Dipole-Bound Anions of Highly Polar Molecules: Ethylene Carbonate and Vinylene Carbonate. *J. Chem. Phys.* **2004**, *120*, 685−690.
(34) Belogolova, E. F.; Vakul'skaya, T. I.; Sidorkin, V. F. Radical Anions of Hypervalent Silicon Compounds: 1-Substituted Silatranes. *Phys. Chem. Chem. Phys.* **2015**, *17*, 12735−12746.
(35) Smith, D. M. A.; Jalbout, A. F.; Smets, L.; Adamowicz, L. Cytosine Anions: Ab Initio Study. *Chem. Phys.* **2000**, *260*, 45−51.
(36) Sidorkin, V. F.; Doronina, E. P. Cage Silaphosphanes with a P-Si Dative Bond. *Organometallics* **2009**, *28*, 5305−5315.
(37) Csonka, G. I.; Hencsei, P. Ab Initio Molecular Orbital Study of 1-Fluorosilatrane. *J. Comput. Chem.* **1994**, *15*, 385−394.
(38) Schmidt, M. W.; Windus, T. L.; Gordon, M. S. Structural Trends in Silicon Atranes. *J. Am. Chem. Soc.* **1995**, *117*, 7480−7486.

DOI: 10.1021/acs.jpclett.8b00355
J. Phys. Chem. Lett. 2018, 9, 1284−1289